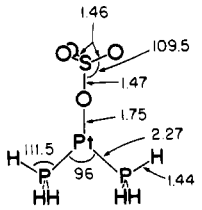

Figure 11. Structure of the product when sulfate is constrained to be monodentate.

on going from a four-membered to a five-membered cyclic structure is 1.9 eV. Our calculations, therefore, suggest that the formation of a four-membered ring is less probable.

Finally, we calculate the structure and stability of monodentate sulfate coordinated to $Pt(PH_3)_2$. The calculated structure is shown in Figure 11. The binding energy of SO_2 with the dioxygen complex to form monodentate sulfate is 4.9 eV, showing that it is 0.6 eV less stable than the bidentate sulfate structure, as expected on the basis of the structure of molecular sodium sulfates.[13]

Conclusions

We have found sulfate formation from sulfur dioxide and bis(phosphine)platinum proceeds most readily through a five-atom cyclic intermediate, which is similar to the stable pseudo-ozonide that forms when ketones react instead of SO_2. Our finding that the sulfur in SO_2 attacks one end of coordinated O_2 in the initial step suggests the ketone may do the same, rather than first coordinating to an axial Pt site as was suggested.[7] The four-atom cyclic intermediate is eliminated on the grounds that if it does form it transforms to sulfate only with difficulty and its formation is hindered by the necessity of activating the coordinated O_2 ligand.

Acknowledgment. We thank the NASA Lewis Research Center for supporting this work through NASA Grant NAG-3-341.

(13) (a) Anderson, A. B. *Chem. Phys. Lett.* **1982**, *93*, 538. (b) Atkins, R. M.; Gingerich, K. A. *Chem. Phys. Lett.* **1978**, *53*, 347.

Contribution from the Department of Chemistry, Texas A&M University, College Station, Texas 77843

Generalized Molecular Orbital Calculations on Transition-Metal Dioxygen Complexes: Model for Manganese Porphyrin

JAMES E. NEWTON and MICHAEL B. HALL*

Received June 26, 1984

Restricted Hartree–Fock plus configuration interaction and generalized molecular orbital plus configuration interaction calculations are reported for several structural models of the dioxygen complexes of manganese(II) porphyrins. An analysis of the results suggests a ground-state structure with a side-on (Griffith) dioxygen and oxygen atoms eclipsing the ring nitrogens. The calculation predicts three singly occupied metal orbitals ($t_2^2e^1$ in pseudocubic symmetry; $\sigma^1\pi^1\delta^1$ in pseudolinear symmetry) in agreement with the ESR results. In contrast to previous ab initio calculations, the CI results also predict a ground-state end-on (Pauling) structure with three unpaired electrons in metal orbitals that would be consistent with the ESR. On the basis of our calculations alone, this structure could not be eliminated as a possibility.

Introduction

At low temperature the reversible reaction of molecular oxygen with a manganese porphyrin yields a pentacoordinate complex, $Mn(O_2)P$ (P = porphyrin dianion).[1] The deoxygenated manganese porphyrin exists as a high-spin d^5 Mn(II) complex, with a single electron in each of the 3d orbitals. These manganese porphyrins contain a single axial ligand,[2] which is replaced by the O_2 ligand in the manganese–dioxygen porphyrin. Electron paramagnetic resonance (EPR) studies of $Mn(O_2)P$ indicate the presence of three unpaired electrons, and ^{17}O substitution shows that little unpaired spin density resides on the O_2 ligand.[1]

Other manganese complexes that also form dioxygen adducts have as other ligands phthalocyanine,[3-6] catechol,[7] salen,[8] sorbitol,[9] tertiary phosphines,[10] and carbonyls.[11] These complexes normally contain one O_2 ligand per Mn atom, although the monomeric $Mn(O_2)Pc$ (Pc = phthalocyanine) compound is an intermediate in the formation of the μ-oxo dimer.[3,4] Coleman and Taylor have recently reviewed reactivity–structure correlations in these complexes, and Gubelmann and Williams have reviewed both these and related complexes.[12]

Although no crystal structure has been obtained for the manganese dioxygen porphyrin, the ESR and particularly the IR ($^{16}O_2$, $^{18}O_2$, $^{16}O^{18}O$) results[1d] seem best interpreted as a side-on or Griffith geometry (**1**). Formally this would correspond to a peroxo

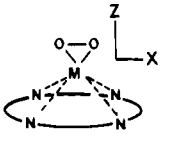

1

complex, $Mn^{4+}O_2^{2-}$. Three reasonably low-energy electronic configurations $[(x^2-y^2)^1(xz)^1(yz)^1]$, $[(x^2-y^2)^1(yz)^1(z^2)^1]$, and $[(x^2-y^2)^1(yz)^1(xy)^1]$ were proposed to provide acceptable solutions to the ESR results. Extended Hückel calculations were reported to favor the $[(x^2-y^2)^1(yz)^1(z^2)^1]$ configuration.[13] However, the

(1) (a) Weschler, C. J.; Hoffman, B. M.; Basolo, F. *J. Am. Chem. Soc.* **1975**, *97*, 5278. (b) Hoffman, B. M.; Weschler, C. J.; Basolo, F. *J. Am. Chem. Soc.* **1976**, *98*, 5473. (c) Hoffman, B. M.; Szymanski, T.; Brown, T. G.; Basolo, F. *J. Am. Chem. Soc.* **1978**, *100*, 7253. (d) Urban, M. W.; Nakamoto, K.; Basolo, F. *Inorg. Chem.* **1982**, *21*, 3406.
(2) (a) Gonzales, B.; Youba, J.; Yee, S.; Reed, C. A.; Kirner, J. F.; Scheidt, W. R. *J. Am. Chem. Soc.* **1975**, *97*, 3247. (b) Kirner, J. F.; Reed, C. A.; Scheidt, W. R. *J. Am. Chem. Soc.* **1977**, *99*, 2557.
(3) (a) Elvidge, J. A.; Lever, A. B. P. *Proc. Chem. Soc.* **1959**, 195. (b) Lever, A. B. P.; Wilshire, J. P.; Quan, S. K. *J. Am. Chem. Soc.* **1979**, *101*, 3668. (c) Lever, A. B. P.; Wilshire, J. P.; Quan, S. K. *Inorg. Chem.* **1981**, *20*, 761.
(4) Watanabe, T.; Ama, T.; Nakamoto, K. *Inorg. Chem.* **1983**, *22*, 2470.
(5) Uchida, K.; Naito, S.; Soma, M.; Onishi, T.; Tamara, K. *J. Chem. Soc., Chem. Commun.* **1978**, 217.
(6) Moxon, N. T.; Fielding, P. E.; Gregson, A. K. *J. Chem. Soc., Chem. Commun.* **1981**, 98.
(7) (a) Magers, K. D.; Smith, C. G.; Sawyer, D. T. *J. Am. Chem. Soc.* **1978**, *100*, 989. (b) Magers, K. D.; Smith, C. G.; Sawyer, D. T. *Inorg. Chem.* **1980**, *19*, 492.
(8) (a) Coleman, W. M.; Taylor, L. T. *Inorg. Chem.* **1977**, *16*, 1114. (b) Chiswell, B. *Inorg. Chim. Acta* **1977**, *23*, 77.
(9) Richens, D. T.; Smith, C. G.; Sawyer, D. T. *Inorg. Chem.* **1979**, *18*, 706.
(10) McAuliffe, C. A.; Al Khateeb, H.; Jones, M. H.; Levason, W.; Minten, K.; McCullough, F. P. *J. Chem. Soc., Chem. Commun.* **1978**, 736.
(11) Fieldhouse, S. A.; Fullam, B. W.; Nielson, C. W.; Symons, M. C. R. *J. Chem. Soc., Dalton Trans.* **1974**, 567.
(12) (a) Coleman, W. M.; Taylor, L. T. *Coord. Chem. Rev.* **1980**, *32*, 1. (b) Gubelmann, M. H.; Williams, A. F. *Struct. Bonding (Berlin)* **1983**, *55*, 1.
(13) (a) Hanson, L. K.; Hoffman, B. M. *J. Am. Chem. Soc.* **1980**, *102*, 4602. (b) Hanson, L. K. *Int. J. Quantum Chem., Quantum Biol. Symp.* **1979**, *6*, 73.

0020-1669/85/1324-2573$01.50/0

Table I. Comparison of Approximate MO Calculations on $Mn(O_2)P$

P = 2			P = 6		
eigenvalue[a]	symmetry	character	eigenvalue[a]	symmetry	character
−6.42	$22a_2$	45% $3d_{xy}$, 40% P	−9.03	$7a_2$	47% $3d_{xy}$, 47% P
−8.18	$27b_1$	39% $3d_{xz}$, 45% O_2 $1\pi_g$, 8% P	−10.39	$11b_1$	39% $3d_{xz}$, 43% O_2 $i\pi_g$, 10% P
−12.79	$34a_1$	47% $3d_{z^2}$, 15% $4p_z$	−14.81	$18a_1$	49% $3d_{z^2}$, 18% $4p_z$, 7% O_2 $i\pi_g$
−15.52	$22b_2$	55% $3d_{yz}$, 16% P	−16.71	$11b_2$	43% $3d_{yz}$, 39% P
−15.56	$21a_2$	70% $1\pi_g$	−17.18	$6a_2$	80% $1\pi_g$, 19% P
−15.66	$20a_2$	24% $1\pi_g$, 76% P	−18.25	$10b_1$	100% P
−189.07	$32a_1$	88% $3d_{x^2-y^2}$	−18.58	$17a_1$	63% $3d_{x^2-y^2}$, 15% P
−22.93	$29a_1$	15% $3d_{z^2}$, 40% P	−21.39	$16a_1$	21% $3d_{z^2}$, 23% $3d_{x^2-y^2}$, 36% POR
−22.11	$22b_1$	29% $3d_{xz}$, 26% $1\pi_g$	−24.22	$8b_1$	50% $3d_{xz}$, 37% $1\pi_g$
−22.11	$16a_2$	15% $3d_{xy}$	−25.42	$4a_2$	49% $3d_{xy}$, 42% POR
−25.23	$24a_1$	50% $3\sigma_g$	−26.99	$14a_1$	74% $3\sigma_g$
−25.87	$15b_2$	79% $1\pi_g$	−27.80	$8b_1$	80% $1\pi_u$, 15% $3d_{yz}$
−26.93	$22a_1$	77% $1\pi_g$	−28.73	$13a_1$	69% $1\pi_u$, 5% $3d_{z^2}$

[a] In eV.

calculations were not of a predictive nature, because there were doubly occupied orbitals higher in energy than singly occupied orbitals.

The only predictive calculations, which were single-determinant Hartree–Fock–Roothaan calculations,[14] obtained an end-on or Pauling geometry with an electronic configuration that placed an unpaired electron in an O_2 $1\pi_g$ orbital. This result is at variance with the ESR results, which showed almost no spin density on oxygen. Considering the importance of configuration mixing in the electronic structure of FeO_2 linkage,[15-17] we believe an accurate description of the $Mn(O_2)P$ complex may also require configuration interaction.

In this work we report the results of generalized molecular orbital (GMO) and configuration interaction (CI) calculations on models of the $Mn(O_2)P$ system in both the Pauling and Griffith geometries.

Theoretical Section

Porphyrin Model. A model ligand system was developed to simulate the porphyrin ring, **2**, because a reduction in the size of this part of the molecule allows us to use a better MnO_2 basis and more extensive CI. Previously we compared various possible systems, $[NH_2]_4^{2-}$ (**3**), $[NHCH_2]_4^{2-}$ (**4**), $[(NH)_2(CH)_3]_2^{2-}$ (**5**), and $[(NH)_2(CH)]_2^{2-}$ (**6**), with **2** by performing approximate molecular orbital (MO) calculations on FeP and $Fe(O_2)P$ where P = **2**–**6**.[17,18] We found that **6** provided a reasonable balance between accuracy and economy. In order to check that **6** was also a reasonable model for the manganese system, we performed calculations on $Mn(O_2)P$, where P = **2** and **6**, in the Griffith geometry. The results for these two calculations are shown in Table I. Generally, the orbitals for the model ligand system **6** are more stable than those of the porphyrin ring **2**, but the relative energies are similar. The characters of the low-lying unoccupied, the singly occupied, and doubly occupied orbitals are very similar. All of the apparently large differences are simply due to the mixing of nearly degenerate orbitals of the same symmetry. These calculations are only meant to illustrate the similarity of ligand **6** to ligand **2** and are not meant to provide definitive results for the actual system. In fact, these calculations predict a singly occupied $1\pi_g$ O_2 orbital, which is inconsistent with the ESR. Interestingly, the order of MO's is identical with that in the previously reported extended Hückel calculations.[13] As in those calculations, the only way to obtain agreement with experiment is to singly occupy orbitals that are more stable than some doubly occupied orbitals.

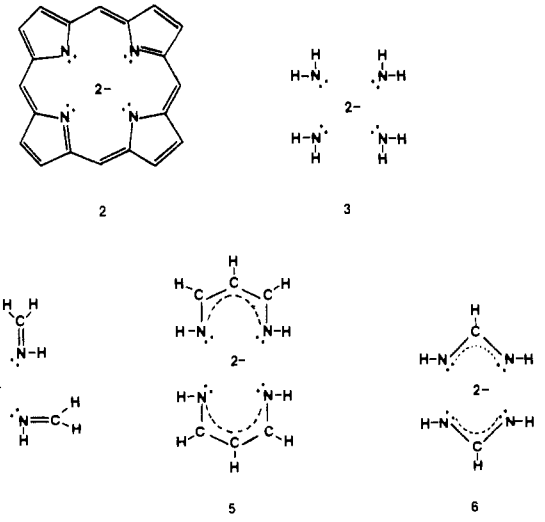

Geometry. The model **6** has N–C, N–H, and C–H bond lengths of 1.40, 0.915, and 1.078 Å, respectively. The N–C–N angle is 125.6°, and the N atoms are placed in the (x,y) plane 2.065 Å from the origin of the coordinate system. Three orientations of the O_2 ligand were considered: **7** is the Pauling geometry, **8** is the Griffith geometry with the O_2 staggered with respect to the N's, and **9** is the Griffith geometry with the O_2 eclipsing the N's.

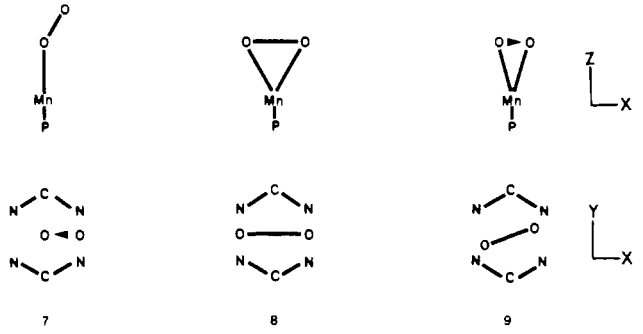

In all of these orientations the Mn was 0.35 Å above the plane of N's, the Mn–O distance was 1.85 Å, and the O–O distance was 1.36 Å, a value between that for superoxide and peroxide ions. For the Pauling geometry, **7**, the Mn–O–O angle was 131°, and for both Griffith geometries this angle was 68.4°. The geometries considered are similar to those of previous studies.[13,14]

Basis Set. The basis set is essentially double ζ for the valence orbitals of manganese and oxygen and minimal for the atoms in the model ligand system. For the GMO–CI calculations the basis

(14) (a) Dedieu, A.; Rohmer, M.-M.; Veillard, A. *Adv. Quantum Chem.* **1982**, *16*, 43. (b) Dedieu, A.; Rohmer, M.-M. *J. Am. Chem. Soc.* **1977**, *99*, 8050. (c) Dedieu, A.; Rohmer, M.-M.; Veillard, H.; Veillard, A. *Nouv. J. Chim.* **1979**, *3*, 653.

(15) (a) Goddard, W. A., III; Olafson, B. D. *Proc. Natl. Acad. Sci. U.S.A.* **1975**, *72*, 2335. (b) Olafson, B. D.; Goddard, W. A., III. *Proc. Natl. Acad Sci. U.S.A.* **1977**, *74*, 1315.

(16) (a) Huynh, B. H.; Case, D. A.; Karplus, M. *J. Am. Chem. Soc.* **1977**, *99*, 1603. (b) Case, D. A.; Huynh, B. H.; Karplus, M. *J. Am. Chem. Soc.* **1979**, *101*, 4433.

(17) Newton, J. E.; Hall, M. B. *Inorg. Chem.* **1984**, *23*, 4627.

(18) Hall, M. B.; Fenske, R. F. *Inorg. Chem.* **1972**, *11*, 768. The basis set and geometry for these calculations is discussed in the M.S. thesis of J. E. Newton, Texas A&M University.

Table II. Total Energies[a] of the RHF–CI and GMO–CI Calculations on **7–9**

calcn	7		8		9	
RHF ($S = {}^7/_2$)	$^8A''$	−1581.011	$^4B_2$	−1580.915	^8B	−1580.908
CI ($S = {}^3/_2$)	$^4A'$	−1580.951	$^4A_1$	−1580.904	^4A	−1580.853
	$^4A''$	−1581.034	$^4A_2$	−1580.83	^4B	−1580.957
			$^4B_1$	−1580.839		
			$^4B_2$	−1580.905		
GMO ($S = {}^3/_2$)	$^4A''$	−1580.857			^4B	−1580.900
CI ($S = {}^3/_2$)	$^4A''$	−1581.007			^4B	−1580.978

[a] In atomic units; 1 au = 27.21 eV.

functions were obtained from a least-squares fit of a linear combination of Gaussians to near-Hartree–Fock-quality Slater-type orbitals.[19] The program, GEXP, processes the functions from the 1s outward, keeping each orbital of higher n quantum number orthogonal to the previous ones. This procedure results in an efficiently nested representation of the functions.[20] The number of Gaussians used for each atomic orbital was increased until the integral error of the fitting was $<10^{-3}$. Three Gaussians per atomic orbital were found to be sufficient for most of the functions. However, a 4-31G type basis was set for the O 2p and a 5-41G type basis was used for the Mn 3d. These were obtained by splitting off the most diffuse component of the fully contracted set. Manganese 4s and 4p functions were included with exponents of 0.20 and 0.25, respectively. This process resulted in a [10s,7p,5d]/(4s,3p,2d) basis for Mn, a [6s,4p]/(2s,2p) basis for O, a [6s,3p]/(2s,1p) basis for C and N, and a [3s]/(1s) basis for H.

Calculations. Both restricted Hartree–Fock–Roothaan (RHF) calculations[21] followed by configuration interaction (CI) calculations[22] and generalized molecular orbital (GMO) calculations[23] followed by CI calculations were used to determine the energy of the various states. In the GMO approach the orbital space is divided into five shells (doubly occupied, strongly occupied, singly occupied, weakly occupied, and unoccupied) rather than the usual three (doubly occupied, singly occupied, and unoccupied). The two new shells, strongly and weakly occupied, represent the orbitals containing electron pairs to be correlated and the orbitals providing that correlation, respectively. The GMO procedure solves for these orbitals with a limited type of multiconfiguration self-consistent-field calculation. The subsequent CI calculation usually includes at least those configurations one can make from single and double excitations out of the strongly occupied into the weakly occupied orbitals. Details of each calculation will be presented with the results.

All calculations were performed on an AMDAHL 470/V6 computer at the Data Processing Center of Texas A&M University. The ATMOL integral–SCF package[24] was modified by addition of the GMO module. The CI calculations were performed with programs written by Dr. C. T. Corcoran, Dr. J. M. Norbeck, and Professor P. R. Certain and modified by T. E. Taylor for the AMDAHL–ATMOL3 system. Orbital plots were prepared by the program MOPLOT.[25]

Results

RHF–CI Results. Initially we performed RHF calculations on the high-spin ($S = {}^7/_2$) states of the $Mn(O_2)P$ model for the three geometries **7**, **8**, and **9**. In these calculations the singly occupied orbitals included the five 3d orbitals of Mn and the two $1\pi_g$ orbitals of O_2. The results are shown in the top of Table II. In the high-spin state the Pauling geometry is over 60 kcal mol^{-1} more stable than either of the Griffith geometries, which differ by less than 4 kcal mol^{-1}.

Table III. The $^4A''$ Ground-State Wave Function for the End-On Geometry, **7**

Wave Function	
$(3d_{z^2} + 1\pi_g{}^3)^2(3d_{yz} + 1\pi_g{}^a)^2(3d_{xz})^1(3d_{x^2-y^2})^1(3d_{xy})^1$	34%
$(3d_{yz} + 1\pi_g{}^a)^2 \rightarrow (3d_{yz} + 1\pi_g{}^a)^1(3d_{yz} - 1\pi_g{}^a)^1$	19%
$(3d_{z^2} + 1\pi_g{}^s)^2(3d_{yz} + 1\pi_g{}^a)^2 \rightarrow (3d_{z^2} + 1\pi_g{}^s)^1(3d_{yz} + 1\pi_g{}^a)^1(3d_{z^2} - 1\pi_g{}^s)^1(3d_{yz} - 1\pi_g{}^a)^1$	14%
$(3d_{z^2} + 1\pi_g{}^s)^2 \rightarrow (3d_{z^2} + 1\pi_g{}^s)^1(3d_{z^2} - 1\pi_g{}^s)^1$	10%
$(3d_{yz} + 1\pi_g{}^a)^2 \rightarrow (3d_{yz} - 1\pi_g{}^a)^2$	9%
$(3d_{z^2} + 1\pi_g{}^s)^2 \rightarrow (3d_{z^2} - 1\pi_g{}^s)^2$	4%
$(3d_{z^2} - 1\pi_g{}^s)^2(3d_{yz} + 1\pi_g{}^a)^2 \rightarrow (3d_{z^2} + 1\pi_g{}^s)^1(3d_{z^2} - 1\pi_g{}^s)^1(3d_{yz} - 1\pi_g{}^a)^2$	4%
$(3d_{z^2} + 1\pi_g{}^s)^2(3d_{yz} + 1\pi_g{}^a)^2 \rightarrow (3d_{z^2} - 1\pi_g{}^s)^2(3d_{yz} - 1\pi_g{}^a)^2$	1%
Natural-Orbital Occupation	
$(3d_{z^2} + 1\pi_g{}^s)^{1.62}(3d_{yz} + 1\pi_g{}^a)^{1.38}(3d_{xz})^{1.00}(3d_{x^2-y^2})^{1.00}$	
$(3d_{xy})^{1.00}(3d_{yz} - 1\pi_g{}^a)^{0.62}(3d_{z^2} - 1\pi_g{}^s)^{0.38}$	

Since the ESR results suggest a $S = {}^3/_2$ ground state, we followed the RHF calculation by a full CI calculation using the seven electrons (five from Mn and two from O) and the seven orbitals that were singly occupied in the RHF calculation. All possible configurations corresponding to $S = {}^3/_2$ were formed, and the lowest root of each symmetry was extracted. The total energies for these states are shown just below the RHF results. For the Pauling geometry, **7**, the $^4A''$ is more stable than either the $^4A'$ or the high-spin $^8A''$. For the Griffith geometry with the dioxygen staggered between N's, all the quartet states are higher in energy than the high-spin $^8B_2$. For the eclipsed Griffith geometry, **9**, the ^4B state is more stable than either the ^4A or the high-spin ^8B. Because all of the quartet states for **8** were higher in energy than the ^4B state of **9**, we eliminated **8** from further consideration. From the lowest energies for **7** and **9**, which are the expected conformations for the Pauling and Griffith geometries,[13,14] we would predict the ground state to be a Pauling geometry of $^4A''$ symmetry. The natural-orbital analysis suggests that the singly occupied orbitals would be xz, $x^2 - y^2$, and xy. However, the quartet energies were determined from orbitals optimized for the high-spin octet states. Therefore, we proceeded to recalculate the energy of the $^4A''$ for **7** and the ^4B for **9** using the GMO–CI approach.

GMO–CI $^4A''$. The seven orbitals that were singly occupied in the RHF calculations were then divided into three shells: strongly occupied, singly occupied, and weakly occupied. The choice of orbitals for these shells was based on the natural-orbital (NO) analysis of the $^4A''$ RHF–CI wave function. The strongly occupied shell included the Mn–O_2 σ bond formed from the Mn $3d_{z^2}$ and O_2 $1\pi_g{}^s$ orbitals[26] and the π bond formed from the Mn $3d_{yz}$ and $1\pi_g{}^a$ orbitals. These two orbitals will be designated $(3d_{z^2} + 1\pi_g{}^s)$ and $(3d_{yz} + 1\pi_g{}^a)$, respectively. Their antibonding counterparts, $(3d_{z^2} - 1\pi_g{}^s)$ and $(3d_{yz} - 1\pi_g{}^a)$, comprise the weakly occupied shell. The $3d_{xz}$, $3d_{x^2-y^2}$, and $3d_{xz}$ orbitals were placed in the singly occupied shell. After cycling to self-consistency, the final wave function was determined from a full CI calculation with the seven electrons distributed in all possible ways in the seven orbitals. The total energies obtained for these calculations are listed in the lower left of Table II. Comparison of the GMO–CI energy with the RHF–CI energy suggests that the GMO step was not successful in improving the orbitals for the CI calculation. The CI wave function, whose largest contributions are listed in Table III, also reflects this problem. Thus, the primary configuration, which places two electrons in both the σ and π Mn–O_2 bonds, is responsible for only 34% of the wave function. Double excitations from these bonding orbitals to their antibonding

(19) Roetti, C.; Clementi, E. *J. Chem. Phys.* **1974**, *60*, 3342.
(20) Marron, M. T.; Handy, M. C.; Parr, R. G.; Silverstone, H. G. *Int. J. Quantum Chem.* **1970**, *4*, 245.
(21) Roothaan, C. J. *Rev. Mod. Phys.* **1951**, *23*, 69; **1960**, *32*, 179.
(22) Shavitt, I. "Methods of Electronic Structure Theory"; Schaefer, H. F., III, Ed.; Plenum Press: New York, 1977.
(23) (a) Hall, M. B. *Chem. Phys. Lett.* **1979**, *61*, 461. (b) Hall, M. B. *Int. J. Quantum Chem.* **1978**, *14*, 613. (c) Hall, M. B. *Int. J. Quantum Chem., Quantum Chem. Symp.* **1977**, *13*, 195. (d) Hall, M. B. In "Recent Developments and Applications of Multiconfiguration Hartree-Fock Methods", NRCC Proceedings No. 10; Dupius, M., Ed.; Lawrence Berkeley Laboratories, National Technical Information Service: Springfield, VA, 1980; p 31.
(24) Guest, M. F.; Hillier, I. H.; Saunders, V. R. ATMOL3 System, Daresbury Laboratory, Warrington WA4 4AD, U.K.
(25) Written by D. L. Lichtenberger, University of Arizona.

(26) The designations "s" and "a" refer to orbitals that are symmetric and antisymmetric with respect to reflection in the MnO_2 plane.

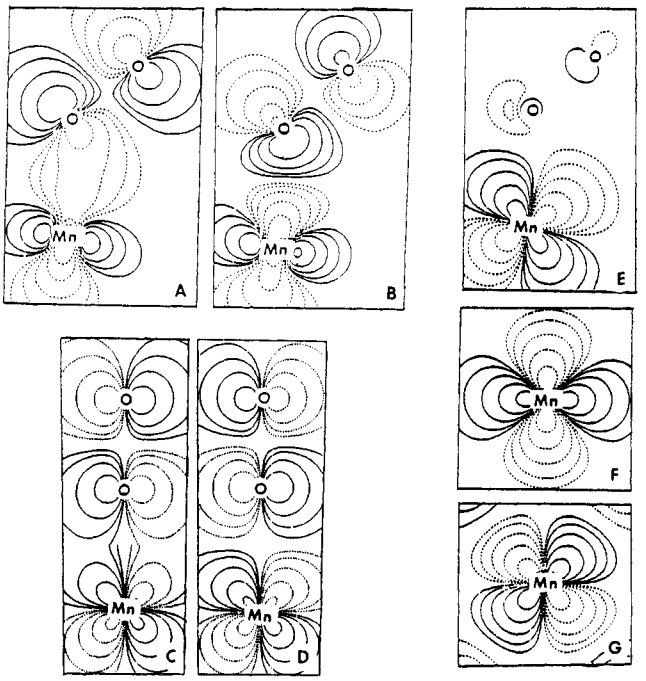

Figure 1. Orbital plots of the natural orbitals from the $^4A''$ state for the end-on Pauling geometry.

counterparts make up 27% of the wave function. These double excitations are primarily involved in the spatial separation (correlation) of the Mn–O σ-bonding and Mn–O π-bonding electron pairs. Single excitations, which would vanish in a complete MCSCF treatment, still make up 29% of our wave function. Previous GMO calculations always reduced the contributions of single excitations to less than a few percent of the wave function. The reason for the different behavior in this case is not clear.

In spite of this computational problem, the wave function for $^4A''$ provides an adequate description of a new possibility for the ground state of the manganese dioxygen porphyrin. The spin coupling of electrons is such that nearly all of the spin density remains on Mn with the $3d_{xz}$, $3d_{x^2-y^2}$, and $3d_{xy}$ orbitals singly occupied. The NO analysis provides the occupation numbers shown at the bottom of Table III. The large occupation numbers for the antibonding orbitals reflect the inadequacy of a simple orbital picture for this state.

Plots of the natural orbitals are shown in Figure 1. The Fe–O_2 bond is shown in Figure 1A, and its antibonding counterpart, in Figure 1B. The bonding and antibonding π orbitals are shown in Figure 1C,D, respectively. The singly occupied orbitals are shown in Figure 1E–G. Note that these are nearly pure Mn 3d orbitals with little or no O_2 character.

GMO–CI ^{4}B. On the basis of the CI results for the lowest energy Griffith geometry, we chose the strongly occupied orbitals to be the in-phase combination of the O_2 $1\pi_g$ orbitals with the appropriate metal d orbital.[27] Thus, the strongly occupied orbitals were the Mn–O_2 π (**10**) and δ (**11**) orbitals ($3d_{xz'} + 1\pi_g^s$; $3d_{x^2-y^2} + 1\pi_g^a$), and the weakly occupied orbitals were the Mn–O_2 π^* (**12**) and δ^* (**13**) orbitals ($3d_{xz'} - 1\pi_g^s$; $3d_{x^2-y^2} - 1\pi_g^a$). The $3d_{z^2}$, $3d_{xy}$, and $3d_{yz'}$ orbitals were singly occupied.

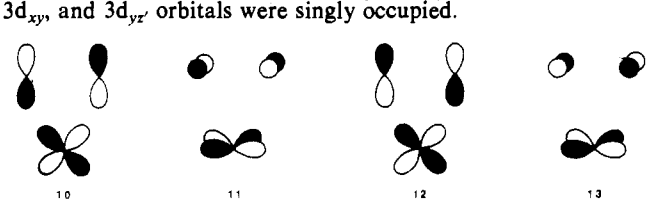

(27) The O_2 ligand in this calculation was rotated about the z axis 45° and now bisects the x and y axes; thus, the contribution from the Mn $3d_{xz}$ and $3d_{yz}$ were mixed to form a $3d_{xz+yz}$ orbital in the plane of the O_2 ligand and a $3d_{xz-yz}$ orbital perpendicular to the former. For convenience, we will employ the notation $3d_{xz'}$ and $3d_{yz'}$ for the $3d_{xz+yz}$ and $3d_{xz-yz}$ orbitals, respectively.

Table IV. The ^{4}B Ground-State Wave Function for the Side-On Geometry, **9**

Wave Function	
$(3d_{z^2} + 1\pi_u^s)^2(3d_{xz'} + 1\pi_g^s)^2(3d_{z^2} - 1\pi_u^s)^1(3d_{yz'})^1(3d_{x^2-y^2})^1$	73%
$(3d_{xz'} + 1\pi_g^s)^2 \rightarrow (3d_{xz'} + 1\pi_g^s)^1(3d_{xz'} - 1\pi_g^s)^1$	11%
$(3d_{xz'} + 1\pi_g^s)^2 \rightarrow (3d_{xz'} - 1\pi_g^s)^2$	7%
$(3d_{z^2} + 1\pi_u^s)^2(3d_{xz'} + 1\pi_g^s)^2 \rightarrow$ $(3d_{z^2} + 1\pi_u^s)^1(3d_{xz'} + 1\pi_g^s)^1(3d_{xz'} - 1\pi_g^s)^1(3d_{xy})^1$	5%
$(3d_{z^2} + 1\pi_u^s)^2 \rightarrow (3d_{xz'} - 1\pi_g^s)^2$	1%

Natural-Orbital Occupation

$(3d_{z^2} + 1\pi_u^s)^{1.93}(3d_{xz'} + 1\pi_g^s)^{1.75}(3d_{z^2} - 1\pi_u^s)^{1.00}(3d_{yz'})^{1.00}$
$(3d_{x^2-y^2})^{1.00}(3d_{xz'} - 1\pi_g^s)^{0.27}(3d_{xy})^{0.05}$

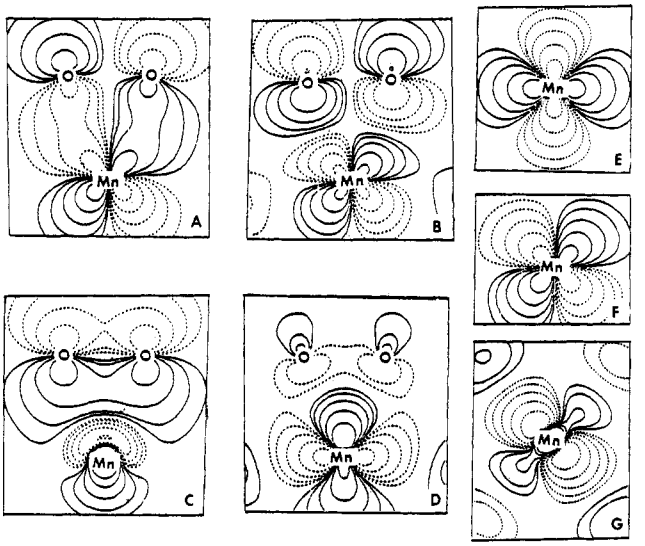

Figure 2. Orbital plots of the natural orbitals from the ^{4}B state for the side-on Griffith geometry.

As the orbitals were optimized, the Mn–O_2 δ and δ^* orbitals rotated into a Mn–O_2 σ and σ^* set (**14** and **15**), created by interaction of the $1\pi_u^s$ orbital with the $3d_{z^2}$ function. The $1\pi_g^a$ orbital replaced the $1\pi_u^s$ orbital in the doubly occupied shell. Further optimization caused the $3d_{x^2-y^2}$ to exchange shells with the singly occupied $3d_{xy}$ orbital.

After self-consistency was attained, the final wave function was again determined from a full CI calculation within the strongly, singly, and weakly occupied orbitals. The resulting total energy is in the lower right of Table II. In contrast to the Pauling geometry, the GMO–CI result is lower in energy than the RHF–CI result, and the wave function of the Griffith geometry appears more like a ground-state wave function. The major configurations are listed in Table IV. The primary configuration is responsible for 73% of the total wave function. The paired excitation of the two electrons from ($3d_{xz'} + 1\pi_g^s$) to ($3d_{xz'} - 1\pi_g^s$) comprises 7% and the paired excitation from ($3d_{z^2} + 1\pi_u^s$) to ($3d_{xz'} - 1\pi_g^s$) is responsible for 1% of the wave function. Configurations with five and seven singly occupied orbitals contribute only 11% and 5%, respectively.

The NO occupation numbers are shown at the bottom of Table IV. The orbitals that were involved in the Mn–O_2 π bond, ($3d_{xz'} + 1\pi_g^s$) and ($3d_{xz'} - 1\pi_g^s$), appear as a NO pair since there is a large transfer of electrons to the latter orbital from the former. However, the $1\pi_g^a$ orbital became doubly occupied rather than participate in a "δ-type" interaction with the metal $d_{x^2-y^2}$ orbital. Thus, a spin-pairing model[28] for the Griffith geometry does not

accurately describe this system. Plots of the natural orbitals are shown in Figure 2.

The orbital in Figure 2A is the π-bonding combination of the Mn atom with the O_2 ligand. The weakly occupied antibonding counterpart is shown in Figure 2B. The σ bond between the Mn $3d_{z^2}$ orbital and the O_2 $1\pi_u^s$ orbital is shown in Figure 2C. This orbital contains an internal node due to the orthogonality of the Mn $3p_z$ function to the $4p_z$, which is used in this orbital. The nonbonding, singly occupied, counterpart (Figure 2D) is centered primarily on the Mn $3d_{z^2}$ function. The doughnut ring of $3d_{z^2}$ function of this orbital is distorted to bond with the O_2 ligand. The three "pure-metal" orbitals are shown in Figure 2E-G. The singly occupied Mn $3d_{x^2-y^2}$ and $3d_{yz}$ orbitals are shown in Figure 2E,F, respectively, and the weakly occupied Mn $3d_{xy}$ orbital is shown in Figure 2G. The lobes of the last orbital are distorted so that they are directed away from the O_2 atoms.

Discussion

The final results for both the Pauling geometry, **7**, and the Griffith geometry, **9**, place the three unpaired electrons in orbitals that are primarily Mn 3d in character. Thus, our results for both yield configurations that can be described in pseudocubic symmetry as "$t_2^2e^1$", in agreement with the ESR spectra.

The GMO-CI results appear to give the impression that the ground-state configuration of manganese-dioxygen porphyrins favor the Pauling geometry. However, the total energies listed in Table II show that neither geometry was favored in all calculations. The difference in the total energies of the GMO-CI calculations of **7** and **9** is 18 kcal mol^{-1}. This difference is small and could be quite different if we had used a different model or a slightly different geometry. Since wave functions for ground states are usually well-behaved, the poor representation of the Pauling geometry by a single configuration and the fact that the high-spin dissociative state is lower in energy than any of the quartet states would seem to preclude this structure from being the ground-state geometry. However, we cannot eliminate the possibility that at a slightly different Pauling geometry the calculations would behave.

Our conclusion, in agreement with both the ESR and IR but in disagreement with the previous ab initio results, is that the most likely ground-state structure is the side-on Griffith geometry. This work represents the first accurate theoretical calculations that show the plausibility of that geometry, and it illustrates the importance of including electron correlation in calculations on metal-dioxygen complexes.

Acknowledgment. This work was supported by grants from the National Science Foundation (CHE79-20993 and CHE83-09936) and the Robert A. Welch Foundation (A-648).

Registry No. $Mn(O_2)P$ (end on), 73066-15-6; $Mn(O_2)P$ (side on), 74077-48-8.

(28) (a) Drago, R. S. *Coord. Chem. Rev.* **1980**, *13*, 353. (b) Drago, R. S.; Corden, B. B.; Zombeck, A. *Comments Inorg. Chem.* **1981**, *1*, 53.

Contribution from the Institut für Anorganische und Analytische Chemie, University of Innsbruck, A-6020 Innsbruck, Austria

Quantum-Chemical Investigations on the Interaction of Alkaline-Earth-Metal Ions with Macrocyclic Compounds

SUPOT V. HANNONGBUA and BERND M. RODE*

Received October 8, 1984

The preferred conformations and the "macrocyclic effect" of the cyclic ligands 1,4,7,10-tetraazacyclododecane and 1,4,7,10-tetraoxacyclodecane and their metal complexes are investigated within the framework of the HF-LCAO-MO method. The results show that the general conformation before and after complexation remains the same (only torsion angles change), i.e. the alternate form for the N_4 and the maxidentate form for the O_4 cyclic ligands. For the factors influencing the "macrocyclic effect", our results indicate the effect of the "prestraining" of the cyclic ligands to dominate in the case of the O_4 ligand. An at least equally important factor for the N_4 ligands is the difference in energy gain by metal binding. The coincidence of metal ion size and ligand ring cavity size affects not only energy consumption upon conformational changes of the ring, being adjusted to the metal ion, but also the amount of energy gain in the binding step.

Introduction

The enhanced stability of the metal complexes of cyclic ligands such as polyamines or polyethers compared to that of their open-chain analogues has been named the "macrocyclic effect".[1] In previous papers,[2,3] we have investigated factors influencing this effect, finding that noncyclic ligands must spend much energy to arrange their donor atoms suitably around the metal ion and will experience steric hindrance during this process.[4,5]

Quantitative stereochemical considerations have led to a better understanding of such factors as ring size effects, steric interaction, and flexibility and their energetic consequences. It is generally accepted, that the stability and selectivity of cyclic ligand complexes depend on the ligand's ability to adjust itself to the electronic and geometrical requirements of the metal and on the relation between the size of the metal ion and the ring cavity of the ligand.[6-13]

Until now, no theoretical study on a series of macrocyclic complexes with mono- and divalent cations has been performed. We have investigated, therefore, the effect of both metal ion size

(1) Cabbiness, D. K.; Margerum, D. M. *J. Am. Chem. Soc.* **1969**, *91*, 6540.
(2) Rode, B. M.; Hannongbua, S. V. *Inorg. Chim. Acta* **1984**, *96*, 91.
(3) Reibnegger, G. J.; Rode, B. M. *Inorg. Chim. Acta* **1983**, *72*, 64.
(4) Fabbrizzi, L.; Paoletti, P.; Clay, R. M. *Inorg. Chem.* **1978**, *17*, 1042.
(5) McDougall, G. J.; Handcock, R. D.; Boeyens, J. C. A. *J. Chem. Soc., Dalton Trans.* **1978**, 1438.
(6) Wipff, G.; Weiner, P.; Kollman, P. *J. Am. Chem. Soc.* **1982**, *104*, 3249.
(7) Haymore, B. L.; Lamb, J. D.; Izatt, R. M.; Christensen, J. J. *Inorg. Chem.* **1982**, *21*, 1598.
(8) Lamb, J. D.; Izatt, R. M.; Swain, C. S.; Christensen, J. J. *J. Am. Chem. Soc.* **1980**, *102*, 475.
(9) Anichini, A.; Fabbrizzi, L.; Paoletti, P. *J. Chem. Soc., Dalton Trans.* **1978**, 577.
(10) Hung, Y.; Martin, L. Y.; Jackels, S. C.; Tait, A. M.; Busch, D. H. *J. Am. Chem. Soc.* **1977**, *99*, 4029.
(11) Kodama, M.; Kimura, E. *J. Chem. Soc., Dalton Trans.* **1976**, 2335.
(12) Jones, T. E.; Zimmer, L. L.; Diaddario, L. L.; Rorabacher, D. H. *J. Am. Chem. Soc.* **1975**, *97*, 7163.
(13) Martin, Y. T.; Dehayes, L. J.; Zompa, L. J.; Busch, D. H. *J. Am. Chem. Soc.* **1974**, *96*, 4046.

0020-1669/85/1324-2577$01.50/0